Original Article

Histological Study on the Possible Therapeutic Efficacy of Topical Adipose Tissue Derived Mesenchymal Stem Cells in Experimentally Induced Dry Eye in Male Albino Rats

Amal Ahmed Farag[1], Aliaa Ahmed Farag[2] and Asmaa Ahmed El-Shafei[1]

[1]Department of Histology, [2]Department of ophthalmology, Faculty of Medicine, Cairo University, Egypt

ABSTRACT

Introduction: Dry eye disease (DED) is a prevalent ocular disorder characterized by tear film instability, inflammation, and damage to the ocular surface, often resulting in discomfort and impaired vision. Current therapies primarily offer symptomatic relief, underscoring the need for regenerative approaches.

Aim of the Work: This study aimed at investigating the possible therapeutic effect of topical adipose tissue derived MSCs (ADMSCs) in benzalkonium chloride (BAC) induced dry eye in male albino rat model.

Material and Methods: Thirty-two adult male albino rats were divided into control and experimental groups. DED was induced using topical BAC. The treatment group received a topical dose of ADMSCs (1×10^5 cells in 25 µl) in right eye once daily for one week. Disease induction and therapeutic response were assessed by corneal fluorescein staining, histological examination (H&E staining), and alcian blue staining for goblet cells. Immunohistochemical analyses for TNF-α and PCNA were performed, alongside morphometric and statistical evaluations.

Results: BAC-induced DED resulted in significant corneal epithelial damage, stromal disorganization, basement membrane disruption, goblet cell loss, and lacrimal gland degeneration, accompanied by increased collagen deposition and elevated TNF-α expression. ADMSCs treatment markedly restored corneal and conjunctival architecture, improved goblet cell density, reduced stromal inflammation, and promoted acinar regeneration in the lacrimal gland. Histochemical analysis confirmed partial restoration of collagen organization and glycosaminoglycan content. Immunohistochemistry revealed enhanced epithelial and acinar proliferation (increased PCNA) and decreased TNF-α expression, indicating reduced inflammation. Morphometric analysis showed significant improvements in corneal thickness and goblet cell count in the ADMSC-treated group compared to untreated DED.

Conclusion: Topical ADMSCs therapy effectively ameliorated BAC-induced dry eye histopathological alterations in rats by promoting tissue regeneration and modulating inflammation. These findings supported the potential of ADMSCs as promising regenerative treatment for DED.

Received: 11 June 2025, **Accepted:** 23 June 2025

Key Words: ADMSCs, BAC-induced model, conjunctiva, cornea, dry eye disease, lacrimal glands, TNF-α, PCNA.

Corresponding Author: Asmaa Ahmed El-Shafei, MD, Department of Histology, Faculty of Medicine, Cairo University, Egypt, **Tel.**: +20 10 9014 7994, **E-mail:** asmaashafei@kasralainy.edu.eg

ISSN: 1110-0559, Vol. 48, No. 3

INTRODUCTION

Dry eye disease (DED) is a very common multifactorial disease worldwide. It is characterized essentially by tear film hyperosmolarity, immune dysregulation, neuro-immune interactions, which contribute to inflammation and impairment at the ocular surface. A major contributory factor in DED is the inadequacy of the aqueous tears mainly from the lacrimal gland, causing an electrolyte-mucin-protein imbalance that may potentially injure the conjunctive, corneal epithelium and nerve fibers[1].

Benzalkonium chloride (BAC) is a widely used preservative in ophthalmic eye drops because of its potent antimicrobial properties; however, it is also well recognized for its cytotoxic effects on the ocular surface. BAC acts as a detergent, and repeated exposure can damage the conjunctival and corneal epithelial cells, leading to irritation, chronic inflammation, and symptoms characteristic of DED, such as ocular discomfort, pain, tear film instability, and visual impairment[2]. These symptoms can significantly impair daily activities, including reading and driving, and are associated with increased anxiety and depression in affected individuals[3].

The primary objective in managing DED is to restore the ocular surface and the tear film to its normal state of homeostasis. Unfortunately, most of the commercially available drugs, such as artificial tears, mucin secretagogues, corticosteroids, antibiotics, and NSAIDs, are mainly used to alleviate the symptoms of the disease rather than curing it[4].

Recent research highlighted the potential effectiveness of MSCs in treating conditions such as dry eye disease, limbal stem cell deficiency and corneal transplantation

DOI: 10.21608/ejh.2025.393367.2283

rejection[5]. The therapeutic effects of MSCs are mediated through paracrine signaling, in which they secrete a variety of trophic factors and cytokines that help in the facilitation of tissue repair and immune response modulation. This could particularly be useful in ocular inflammatory diseases where MSCs can assist in restoring homeostasis and promoting healing[6].

MSCs are about 20–30μm in diameter and they have adhesion molecules like CD94d on their surface. Therefore, systemic administration of MSCs can result in the entrapment of these cells in the lungs, thus restricting their therapeutic potential. Topical delivery is a simple and non-invasive approach that applies stem cells directly to the injured cornea. MSCs can adhere to the ocular surface, which makes them suitable for topical application[7].

The present work aims at investigating the possible therapeutic effect of topical adipose tissue derived MSCs (ADMSCs) in benzalkonium chloride (BAC) induced dry eye in male albino rat model. The efficacy of ADMSCs will be monitored by histological, immunohistochemical and morphometric studies.

MATERIAL AND METHODS

Drugs

Benzalkonium chloride (BAC) was purchased from El-Gomhoria chemicals company (Cairo, Egypt) in the form of 500 ml, 50% solution.

Animals

This study was carried out on 34 adult male albino rats, approximately 3 months old. Their body weight ranged between 200 and 250 grams. They were kept in the animal house of Kasr Al-Ainy, Faculty of Medicine, Cairo University, in stain-steel cages under standard environmental conditions with free access to standard diet and water throughout the experimental period. The study protocol was approved by the Institutional Animal Care and Use Committee at Cairo University (IACUC) under the approval number CU III F 6 23.

Experimental design

Rats were divided at random into:

Donor group (n:2): rats were used for ADMSCs isolation, culture, phenotyping and labeling.

Group I (Control group) (n:10): each rat received 0.9% saline drops (the vehicle of BAC) twice daily to the right ocular surface for one week, then rats were randomly subdivided into 2 subgroups:

- Subgroup I-a (n:5): from day 8, rats were left untreated for one week.
- Subgroup I-b (n:5): from day 8, a single drop of PBS (the vehicle of ADMSCs) was topically applied once daily to the conjunctival sac of the right eye of each rat for one week.

Rats of control subgroups were sacrificed with the corresponding experimental subgroups.

Group II (Experimental group (n.22): each rat received 0.2% benzalkonium chloride (BAC) drops twice daily to the right ocular surface for one week[8]. After the establishment of dry eye by fluorescein staining test, rats were randomly subdivided into 2 subgroups:

- Subgroup II-a (Untreated dry eye subgroup: n.10): Starting on day 8, rats were left untreated for one week to assess spontaneous recovery.
- Subgroup II-b (ADMSCs treated subgroup: n.12): Starting on day 8, rats received topical treatment consisting of a 25 μl drop (containing 1×10^5 ADMSCs suspended in PBS) applied once daily to the conjunctival sac of the right eye for one week[9]. To ensure adequate contact time between the therapeutic solution and the ocular surface, we gently held each rat in a secure, upright position for 30–45 seconds after administering the drop. This brief restraint prevented immediate blinking or head-shaking that could displace the solution[10]. Two rats were sacrificed after 3 days to trace SCs and ensure their homing into the cornea, conjunctiva and lacrimal glands[11].

Corneal fluorescein staining test

The ocular surface is assessed for dry eye by applying fluorescein dye. Using 1–2 μl of 2% fluorescein mixed with 10 μl of tears results in a surface concentration of 0.2%, which is optimal for effective staining. A drop of fluorescein is placed on a moistened sterile paper strip, which is then applied to the inner surface of the lower eyelid along with a topical anesthetic. Under cobalt blue light illumination, areas of the cornea that appear bright green indicate the presence of dry eyes. The Fluorescein staining test was performed before and after one week of BAC application to confirm dry eye and after one week of therapy with ADSCs[12].

Standard corneal fluorescein staining scoring system[13]

The Oxford Grading Scale is widely used for grading corneal fluorescein staining. It is semi-quantitative and employs a 0–4 scale for animal studies, Scoring Criteria (0–4 scale):

- **Score 0:** No staining (intact epithelium).
- **Score 1:** Minimal staining, involving less than 25% of the corneal surface; typically, 1–5 punctate spots.
- **Score 2:** Mild staining, 25–50% of the corneal surface; 6–30 punctate spots or small coalescent areas.
- **Score 3:** Moderate staining, 50–75% of the corneal surface; larger coalescent areas.

- **Score 4:** Severe staining, more than 75% of the corneal surface; extensive coalescent staining, possibly with epithelial defects or ulcers.

In Vitro Studies

Isolation and propagation of ADMSCs from rats

At the Tissue Culture Unit of Histology Department, Faculty of Medicine, Cairo University, the rats were euthanized using carbon dioxide, and adipose tissue was collected from their abdominal region. The obtained adipose tissue was thoroughly washed with a saline solution and then incubated for 40 minutes at 37 °C in a DMEM solution supplemented with 1% penicillin-streptomycin and 0.2% collagenase (GIBCO/BRL). Following the defined incubation time, the resultant cell suspension was centrifuged at 630 g for 10 minutes to yield the stromal vascular fraction (SVF). Mononuclear cells were separated by a density gradient centrifugation with Ficoll/Paque. Isolated cells were re-suspended in medium added with 1% of penicillin-streptomycin and placed for culturing at 37 °C in an atmosphere containing 5% CO_2 for 12 to 14 hours. When the confluence of cell colonies reached 80-90%, they were washed twice with PBS, thereafter, treated with 0.25% trypsin in 1 ml of EDTA. Following centrifugation at 2400 rpm for 20 min, the cells were re-suspended in a serum-supplemented medium and transferred to 50 cm^2 Falcon culture flasks. On day 14, the trypsinized colonies were counted and considered as first-passage cultures[14].

Characterization and labeling of ADMSCs[15]

At the end of the third passage, trypsinized adherent cells were counted and diluted to a density of 1×10^6 cells/ml with a hemocytometer. These cells were incubated with 10 µl of monoclonal CD44 antibody (Beckman Coulter, USA) in the dark at a temperature of 4 °C for 20 minutes. Following this incubation time, 2 ml of PBS containing 2% fetal bovine serum (FBS) was added to each tube containing the treated cells. The mixture was centrifuged at 2500 rpm for 5 minutes; the supernatant was removed, and the cells were re-suspended in 500 µl of PBS containing 2% FBS. Cells were analyzed using a CYTOMICS FC 500 Flow Cytometer (Beckman Coulter, FL, USA) and data was analyzed using CXP Software version 2.2. Immunohistochemical detection of CD45 and CD90 was carried out using the streptavidin immune-peroxidase method. At passage four, ADMSCs were harvested and labeled with green fluorescent protein (GFP) for observation under a fluorescent microscope.

At the end of the experiment, all remaining rats were sacrificed by decapitation under the lethal dose of general anesthesia administered via intraperitoneal (ip) injection of 100 mg/kg of a ketamine-xylazine combination[16]. The right eyes were then enucleated, and right lacrimal glands were dissected and preserved in 10% formol saline for a duration of 48 hours. Subsequently, paraffin blocks and sections measuring 5 µm in thickness were prepared for subsequent histological studies:

1. Fluorescent microscopy to trace GFP labeled ADMSCs (Sigma, USA, Catalog Number MIN126) and ensure their homing into the cornea, conjunctiva and lacrimal glands[11].
2. Hematoxylin and eosin stain (H&E)[17] to demonstrate morphological changes in the cornea, conjunctiva, and lacrimal glands.
3. Histochemical stains[18]:
    a. Masson's trichrome stain to detect collagen deposition within the cornea and lacrimal glands.
    b. Alcian Blue-Periodic acid-Schiff (AB-PAS) stain to detect changes in the corneal stroma and membranes, as well as conjunctival goblet cell secretion. Alcian Blue (AB) mainly stains acidic mucins in deep blue color, whereas Periodic Acid-Schiff (PAS) detects neutral mucins in magenta-red.
    c. Periodic acid-Schiff (PAS) stain to demonstrate the lacrimal gland granules and basement membranes.
4. Immunohistochemical staining using the avidin-biotin peroxidase complex technique[19], with 1ry antibodies including: (a) anti-PCNA antibody [PC10] as a marker of proliferation[20] (Catalog # ab29; Abcam, Egypt). (b) anti-TNF-α antibody as a marker of inflammation[21] (Catalog # 4T10; HyTest Ltd., Finland).

For immunohistochemical staining, sections were subjected to antigen retrieval in 10 mM citrate buffer (pH 6) for 10 minutes, then were incubated overnight with primary antibodies. Immunoreactivity was visualized with DAB and counterstained using Mayer's hematoxylin. A small intestine specimen was used as the positive tissue control for PCNA and the positive cells showed nuclear immunoreactivity. Similarly, a lung specimen was used as the positive tissue control for TNF-α and the positive cells demonstrated cytoplasmic or/and nuclear immuoreactivity. Conversely, sections of the cornea, conjunctiva, and lacrimal gland were used as the negative tissue control by omitting the primary antibody step during the staining procedure.

Morphometric study

Data were collected utilizing the "Leica Qwin 500C" image analysis computer system (Leica Imaging System Ltd, Cambridge, UK). In the Histology department, tissue slides were examined under a light microscope, and several parameters were quantified across ten non-overlapping randomly selected fields (at 100x magnification, with a measuring frame of 116964.91 μm^2) for each specimen. The specific parameters measured included:

a. The mean central corneal thickness in sections stained with H & E.

b. The area percentage (%) of collagen in Masson's trichrome stained sections.

c. The number of conjunctival goblet cells in sections stained with PAS-AB.

d. The area % of positive immune expression for PCNA and TNF-α.

Statistical analysis

Data were analyzed using SPSS version 16 (SPSS Inc., Chicago, USA). One-way ANOVA followed by Tukey's post hoc test was used to compare groups. Results are presented as mean ± SD, with statistical significance set at $p<0.05$[22].

RESULTS

No deaths were reported during the experiment. The two subgroups (I-a & I-b) had similar results, so they are collectively called group I (control group).

Corneal fluorescein staining results

In Group I (control group), minimal and focal fluorescein staining was observed, limited to the peripheral cornea (Figure 1A). This pattern indicates an intact and healthy corneal epithelium with no significant epithelial disruption, consistent with a staining grade of 0–1 on standard grading scales. In contrast, Group II (experimental dry eye group) exhibited marked, diffuse fluorescein staining covering a large area of the corneal surface, including central and paracentral regions (Figure 1B). This reflects significant corneal epithelial damage and barrier dysfunction, characteristic of severe dry eye, consistent with a staining grade of 3–4. Subgroup II-a (untreated dry eye) showed moderate, focal fluorescein staining that was less intense than the main dry eye group (Figure 1C). This demonstrates incomplete restoration of epithelial integrity, with residual areas of damage, consistent with a staining grade of 1–2. Finally, Subgroup II-b (ADMSCs treated subgroup) presented minimal, peripheral staining, with most of the corneal surface appearing clear (Figure 1D). This nearly resembles the control group and indicates significant healing of the corneal epithelium along with restoration of its barrier function, consistent with a staining grade of 0–1.

Histological results

Immunofluorescent stained sections

Subgroup II-b (ADMSCs treated subgroup) displayed intensely labeled GFP-retaining stem cells (SCs) in the cornea localized on the surface (Figure 1E), also in the conjunctiva (Figure 1F) and lacrimal gland (Figure 1G); they appear scattered within the stromal and glandular compartments.

Hematoxylin and eosin-stained sections

As regards corneal sections, group I (control) exhibited apparently normal corneal architecture, featuring a non-keratinized stratified squamous epithelium anchored to a uniform intact basement membrane. The substantia propria demonstrated regularly arranged collagen bundles with interspersed quiescent keratocytes. The Descemet's membrane appeared homogenous, acidophilic continuous layer, supporting an intact lining of flattened endothelial cells. (Figure 2A).

In subgroup II-a (untreated dry eye), corneal sections marked histopathological alterations; most of epithelial cells showed dark pyknotic nuclei and cytoplasmic vacuolations, in addition to areas of pronounced separation from underlying stroma with irregular disrupted basement membrane. The substantia propria showed disrupted and separated collagen bundles with some keratocytes exhibiting a slightly rounded or swollen appearance. Descemet's membrane demonstrated focal discontinuities accompanied by endothelial cell loss (Figure 2B).

In subgroup II-b (ADMSCs treated), corneal sections revealed partial restoration of the epithelial layer, with residual scattered vacuolated cells with dark pyknotic nuclei, alongside an intact regular basement membrane. The substantia propria appeared mostly organized with apparently normal keratocytes, although some areas showed collagen separation. Descemet's membrane appeared continuous accompanied by an intact layer of flattened endothelial cells in most regions (Figure 2C).

As regards conjunctiva, group I exhibited apparently normal conjunctiva, showing stratified columnar epithelium with abundant goblet cells and an underlying loose connective tissue (C.T) stroma (Figure 2D). Subgroup II-a showed disrupted conjunctival epithelium with reduced goblet cells. The underlying C.T revealed abundant mononuclear cellular infiltration, most probably inflammatory cells (Figure 2E). In subgroup II-b, more-organized epithelium with visible goblet cells apart from a few distorted areas was detected. The C.T showed a few mononuclear cells (Figure 2F).

As regards lacrimal glands sections, group I showed apparently normal glandular structure exhibiting densely packed serous acini composed of tightly packed pyramidal epithelial cells with central rounded vesicular nuclei and basophilic cytoplasm. Additionally, both intralobular and interlobular ducts were observed, lined by cuboidal epithelial cells with acidophilic cytoplasm (Figure 3A).

Subgroup II-a exhibited significant histological alterations, including structural distortion of acini. Affected acinar cells displayed pyknotic nuclei and cytoplasmic vacuolation. The duct system demonstrated epithelial cell detachment and exfoliation in many ducts, accompanied by vascular congestion within the glandular stroma (Figure 3B).

Subgroup II-b exhibited notable restoration of the acinar architecture, with most acinar cells exhibiting rounded vesicular nuclei, although few cells retained dark pyknotic nuclei alongside cytoplasmic vacuolations. The ductal structures showed incomplete epithelial reorganization, characterized by residual areas of cellular

detachment. Additionally, vascular congestion remained evident (Figure 3C).

Histochemical stained sections

a. Masson's trichrome-stained sections: In corneal sections, group I demonstrated well-organized collagen bundles within the substantia propria, accompanied by regular intact basement and Descemet's membranes (Figure 4A). In contrast, subgroup II-a exhibited disruption and significant separation of collagen bundles in the substantia propria, alongside discontinuities in both basement and Descemet's membranes (Figure 4B). Subgroup II-b displayed mild separation of collagen bundles in substantia propria, in addition to continuous basement and Descemet's membranes (Figure 4C).

In the examined lacrimal gland sections, group I exhibited a normal lobular structure with delicate collagen fibers present in the connective tissue septa and between the acini (Figure 4D). In contrast, subgroup II-a showed a marked increase in collagen deposition, particularly around the ducts and within the interlobular septa, as well as between the acini (Figure 4E). Subgroup II-b displayed a mild to moderate deposition of collagen within the septa and between the acini (Figure 4F).

b. AB-PAS-stained sections: In corneal sections, group I exhibited a strong continuous PAS positivity in both basement and Descemet's membranes, characterized by magenta red color. Concurrently, a strong widespread Alcian blue (AB) positivity was observed in the corneal stroma with a bluish-green hue (Figure 5A). In contrast, subgroup II-a displayed an interrupted PAS positivity in the basement and Descemet's membranes, accompanied by a weak AB positivity in the stroma (Figure 5B). Conversely, subgroup II-B demonstrated a strong, continuous PAS positivity in the basement and Descemet's membranes with a moderate widespread AB positivity in the stroma (Figure 5C).

As regards conjunctiva, group I exhibited numerous alcian blue stained goblet cells within the conjunctival epithelium (Figure 5D). In contrast, subgroup II-a, conjunctival sections revealed a significant reduction in the number of goblet cells (Figure 5E). While subgroup II-b showed a notable increase in goblet cell number within the conjunctival epithelium (Figure 5F).

c. PAS-stained sections: Regarding lacrimal gland sections, group I exhibited well-defined acini characterized by strong PAS-positive granules concentrated in the apical cytoplasm. Furthermore, the basement membranes surrounding these acini, displayed continuous PAS positivity, manifesting as delicate magenta delineations (Figures 6A,D). Conversely, subgroup II-a showed numerous acini with architectural distortion, sparse PAS-positive granules, and discontinuous basement membranes (Figures 6B,E). In contrast, subgroup II-b demonstrated predominantly regenerated acini displaying strong PAS-positive granulation and intact basement membranes (Figures 6C,F).

Immunohistochemical stained sections

a. PCNA immunostained sections: Group I demonstrated negligible PCNA immunoreactivity across the cornea, conjunctiva, and lacrimal glands (Figures 7A,D,G respectively). In subgroup II-a, a moderate increase in PCNA-positive nuclei was observed, predominantly within the basal and supra-basal layers of both corneal and conjunctival epithelia, as well as in the acinar cells of the lacrimal glands (Figures 7B,E,H respectively). Conversely, subgroup II-b showed a marked increase in PCNA-positive nuclei distributed extensively throughout the corneal and conjunctival epithelial layers, corneal keratocytes, and lacrimal gland acinar cells (Figures 7C,F,I respectively).

b. TNF-α immunostained sections: In the examined corneal sections, group I displayed only very faint brown TNF-α immunostaining limited to the nuclei of few basal and supra-basal epithelial cells (Figure 8A). In contrast, subgroup II-a exhibited intense brown cytoplasmic and nuclear TNF-α immunoreactivity within both epithelial and stromal compartments, including keratocytes, vascular endothelial cells, and infiltrating mononuclear cells (Figure 8B). Meanwhile, subgroup II-b showed moderate TNF-α expression, primarily localized to the epithelial layer, with minimal involvement of the stromal tissue (Figure 8C).

In conjunctiva, group I showed negative TNF-α immunoreactivity (Figure 8D). Subgroup II-b showed intense cytoplasmic and nuclear TNF-α immunoreactivity prominent in the irregular epithelial cells with numerous strong TNF-α-positive cells in the stroma (Figure 8E). In contrast, subgroup II-b showed moderate and more localized TNF-α immunoreactivity in the epithelial cells that appeared more organized with reduced number of TNF-α positive cells in the stroma (Figure 8F).

In lacrimal gland sections, group I showed nearly no detectable TNF-α immunoreactivity (Figure 8G). In contrast, subgroup II-a displayed strong widespread cytoplasmic immunoreactivity in the acinar cells (Figure 8H), whereas subgroup II-b exhibited a decreased level of immunoreactivity (Figure 8I).

Morphometric results (Figure 9)

The mean central corneal thickness values ± standard deviation (SD) measured in H&E stained sections was (117.04 ± 3.77) in the control group (group I), (215.07 ± 3.25) in the untreated dry eye subgroup (II-a), and (128.39 ± 3.29) in the ADMSCs treated subgroup (II-b). These results show a statistically significant increase in corneal thickness in subgroup II-a compared to both the control and the treated subgroup II-b, while no significant difference was found between the treated subgroup II-b and the control group.

The mean area % of collagen values (± SD) in corneal sections were (166.61 ± 3.77) in group I, (128.71 ± 4.91) in subgroup II-a and (153.59 ± 3.80) in subgroup II-b. These results indicate a significant decrease in collagen

area in subgroup II-a compared to control and subgroup II-b, while no significant difference was observed between subgroup II-b and group I. In lacrimal gland sections, collagen area % was (142.52 ± 2.10) in group I, (263.93 ± 3.09) in subgroup II-a and (193.27 ± 3.98) in subgroup II-b, with both subgroups II-a and II-b showing significant increases compared to group I, but subgroup II-b had a significant decrease compared to subgroup II-a.

The mean number of alcian blue positive goblet cells (± SD) in the conjunctival sections were (60.17 ± 1.75) in group I, (30.33 ± 1.58) in subgroup II-a, and (50.54 ±1.48) in subgroup II-b. The previous values indicated a significant decrease in subgroup II-a compared to control and subgroup II-b, with no significant difference between subgroup II-b and control group.

The mean values of area % of PCNA immuno-positive cells (± SD) in the corneal sections were (2.20% ± 0.42%) in group I, (8.26% ± 1.01%) in subgroup II-a, and (22.71% ± 2.00%) in subgroup II-b. In conjunctival sections, the mean values were (0.80% ± 0.30%) in group I, (13.60 % ± 1.81%) in subgroup II-a, and (31.42 % ± 2.50%) in subgroup II-b. In lacrimal gland sections, the mean values were (0.04% ± 0.00%) in group I, (2.83 % ± 0.14%) in subgroup II-a, and (11.81 % ± 1.40%) in subgroup II-b. The previous values indicated a significant increase in both subgroups, II-a & II-b compared to control, in addition to a significant increase in subgroup II-b compared to subgroup II-a.

The mean values of area % of TNF-α immuno-positive cells (± SD) in the corneal sections were (1.12% ± 0.03%) in group I, (20.45% ± 0.21%) in subgroup II-a, and (10.68 ± 0.09) in subgroup II-b. In conjunctival sections, the mean values were (2.13% ± 0.50%) in group I, (38.71 ± 4.21%) in subgroup II-a, and (17.43% ± 2.94%) in subgroup II-b. In lacrimal gland sections, the mean values were (0.99% ± 0.08%) in group I, (18.44 % ± 0.24%) in subgroup II-a, and (11.53 % ± 0.40%) in subgroup II-b. The previous values indicated a significant increase in subgroup II-a compared to control and subgroup II-b, in addition to a significant increase in subgroup II-b compared to control.

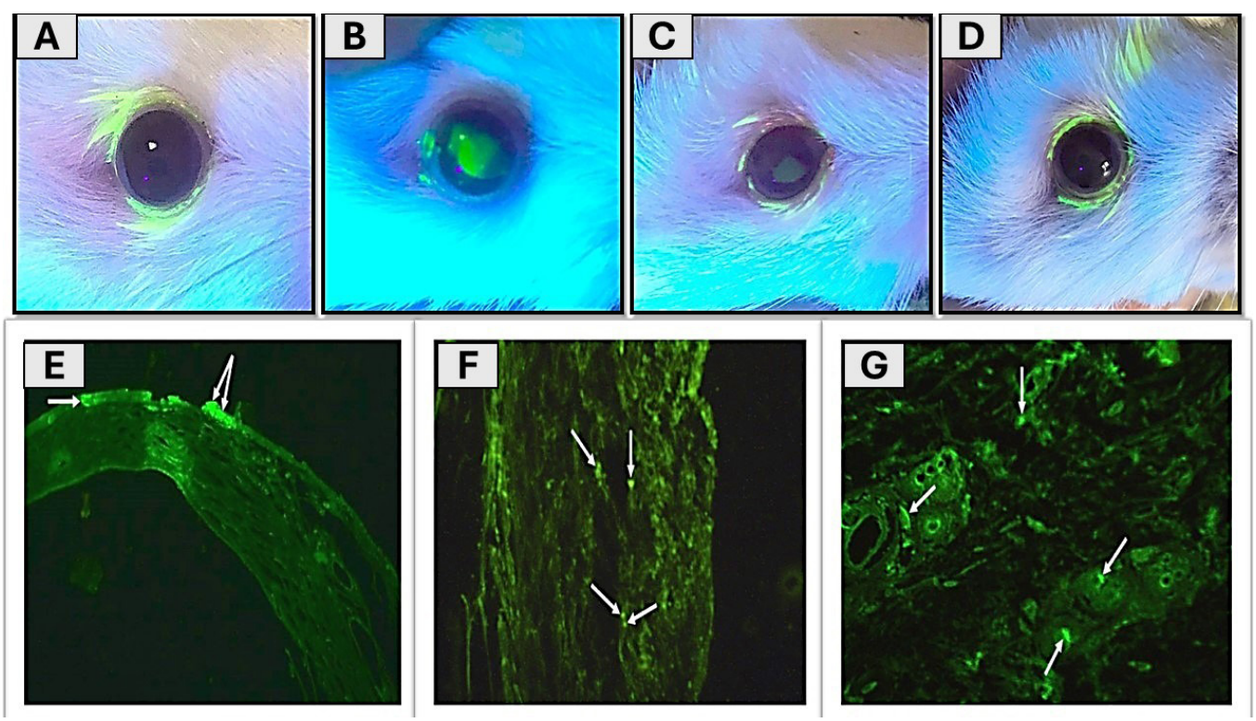

Fig. 1: (A-D) Corneal fluorescein staining; (A) Group I shows minimal peripheral staining. (B) Group II reveals marked diffuse staining. (C) Subgroup II-a displays moderate focal staining. (D) Subgroup II-b shows minimal peripheral staining. (E-G) Photomicrographs of GFP labeled sections of subgroup II-b (x100) demonstrate green positive immunofluorescent stem cells (arrows) housed in the (E) corneal surface, (F) conjunctiva and (G) lacrimal gland.

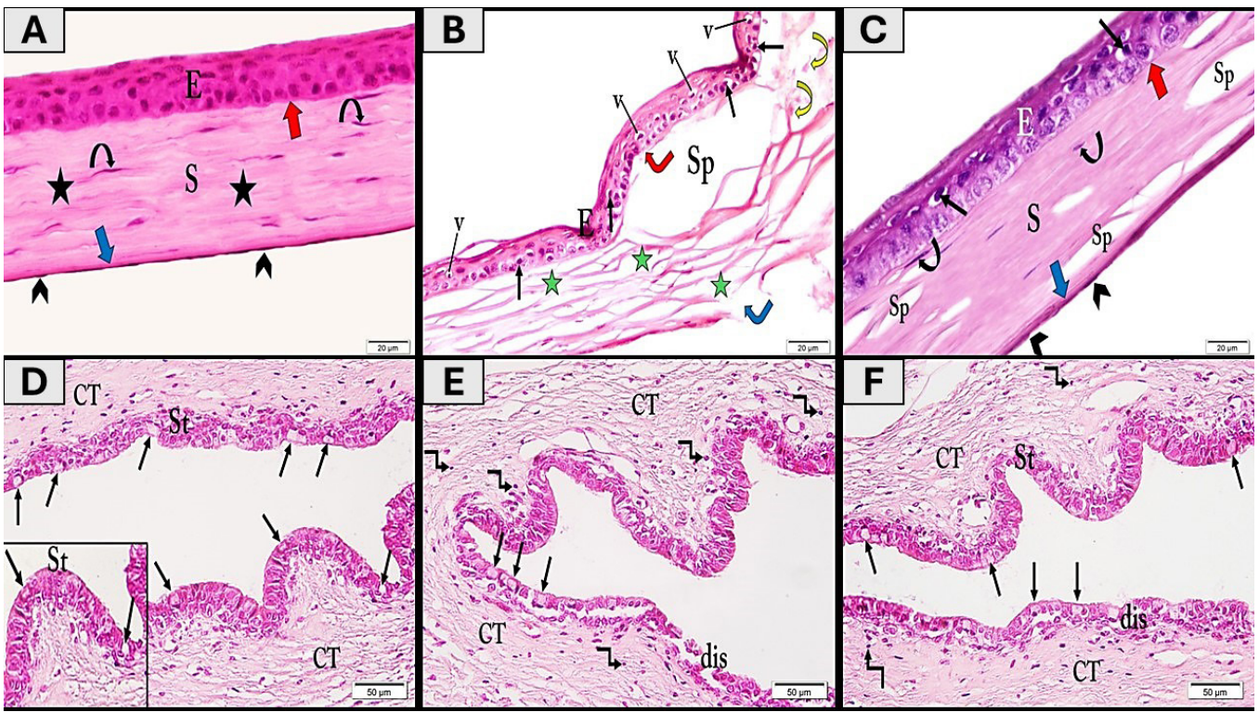

Fig. 2: Photomicrographs of H&E-stained sections of central cornea (x400), conjunctiva (x200). (A, D) Group I demonstrates apparently normal corneal architecture in the form of; non-keratinized stratified squamous epithelium (E) resting on a uniform intact basement membrane (red arrow). The substantia propria (S) shows regularly arranged collagen bundles (stars) with quiescent keratocytes (curved arrows) in between. A homogenous, acidophilic continuous Descemet's membrane (blue arrow) with an intact layer of flattened endothelial cells (arrowheads) are also seen. The conjunctiva shows apparently normal stratified columnar epithelium (St) with numerous goblet cells (arrows) and an underlying loose connective tissue (CT) stroma. (B, E) Subgroup II-a exhibits corneal epithelium (E) with condensed nuclei (arrows) and cytoplasmic vacuolations (v) in most of cells, in addition to areas of pronounced separation (Sp) from underlying stroma with irregular disrupted basement membrane (red right-angled arrow). The substantia propria shows disrupted and separated collagen bundles (green stars) with some slightly rounded or swollen keratocytes (yellow curved arrows) in-between. Focal loss of Descemet's membrane and endothelial cells (blue right-angled arrow) is also noticed. The conjunctiva shows disrupted conjunctival epithelium (dis) with few goblet cells (arrows). The underlying connective tissue (CT) exhibits abundant mononuclear cellular infiltration (right-angled arrows). (C, F) Subgroup II-b shows partial regeneration of corneal epithelium (E) with residual scattered vacuolated cells with condensed nuclei (arrows), alongside an intact regular basement membrane (red arrow). The substantia propria (S) appears mostly organized with apparently normal keratinocytes (curved arrows), although some areas show collagen separation (Sp). A continuous Descemet's membrane (blue arrow) with an intact layer of flattened endothelial cells (arrowheads) are detected. The conjunctiva shows more-organized epithelium (St) with abundant goblet cells (arrows) apart from a few distorted areas (dis) was detected. The connective tissue (CT) showed a few mononuclear cells (right-angled arrows).

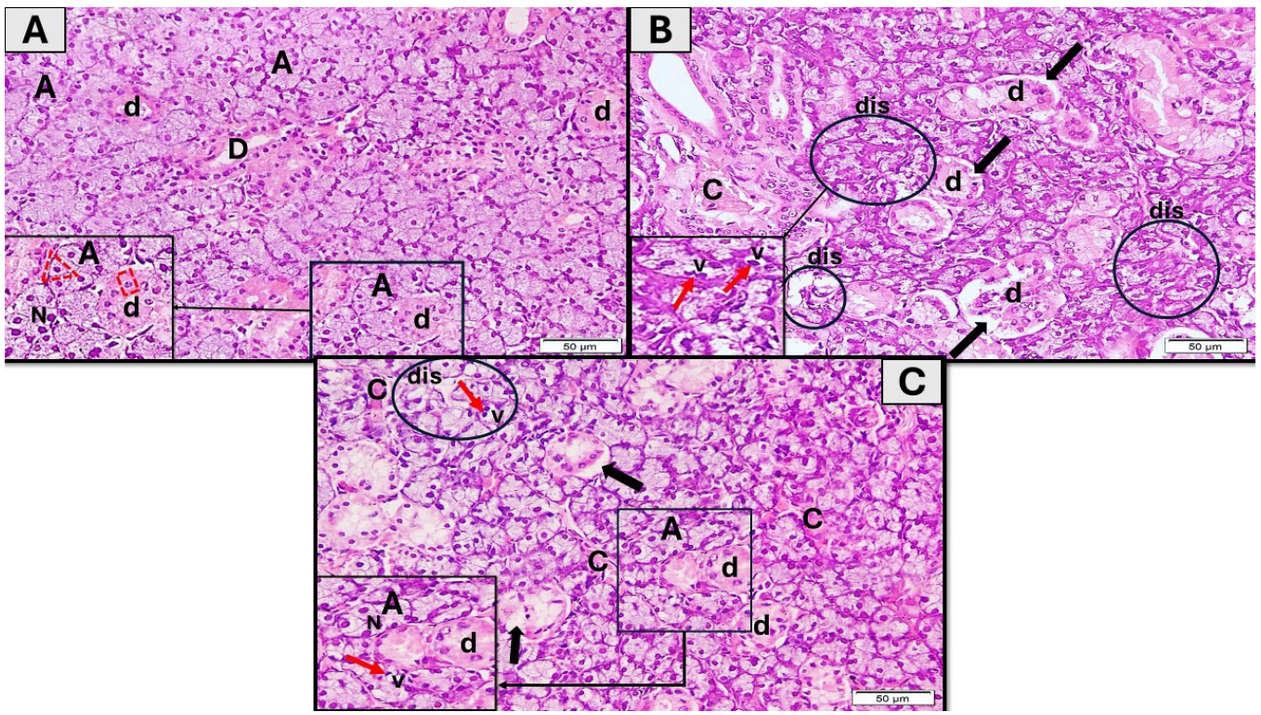

Fig. 3: Photomicrographs of H&E-stained sections of lacrimal glands (x200). (A) Group I shows lacrimal gland shows apparently normal glandular structure exhibiting densely packed serous acini (A) composed of tightly packed pyramidal epithelial cells (triangle) with central rounded vesicular nuclei (N) and basophilic cytoplasm. Additionally, both intralobular (d) and interlobular ducts (D) were observed, lined by cuboidal epithelial cells (rectangle) with acidophilic cytoplasm. (B) Subgroup II-a exhibits lacrimal gland demonstrates areas of acinar distortion (dis). Affected acinar cells display pyknotic nuclei (red arrows) and cytoplasmic vacuolations (v). Many ducts (d) show epithelial cell detachment and exfoliation. A congested vessel (C) within the stroma is also seen. (C) Subgroup II-b shows lacrimal gland exhibits notable restoration of the acinar architecture, with most of acini showing rounded vesicular nuclei (N), although few cells retained dark pyknotic nuclei (red arrows) surrounded by cytoplasmic vacuolations (v). some ducts (d) are apparently normal apart from others with residual areas of cellular detachment (black arrows). Additionally, vascular congestion (C) is still noticed.

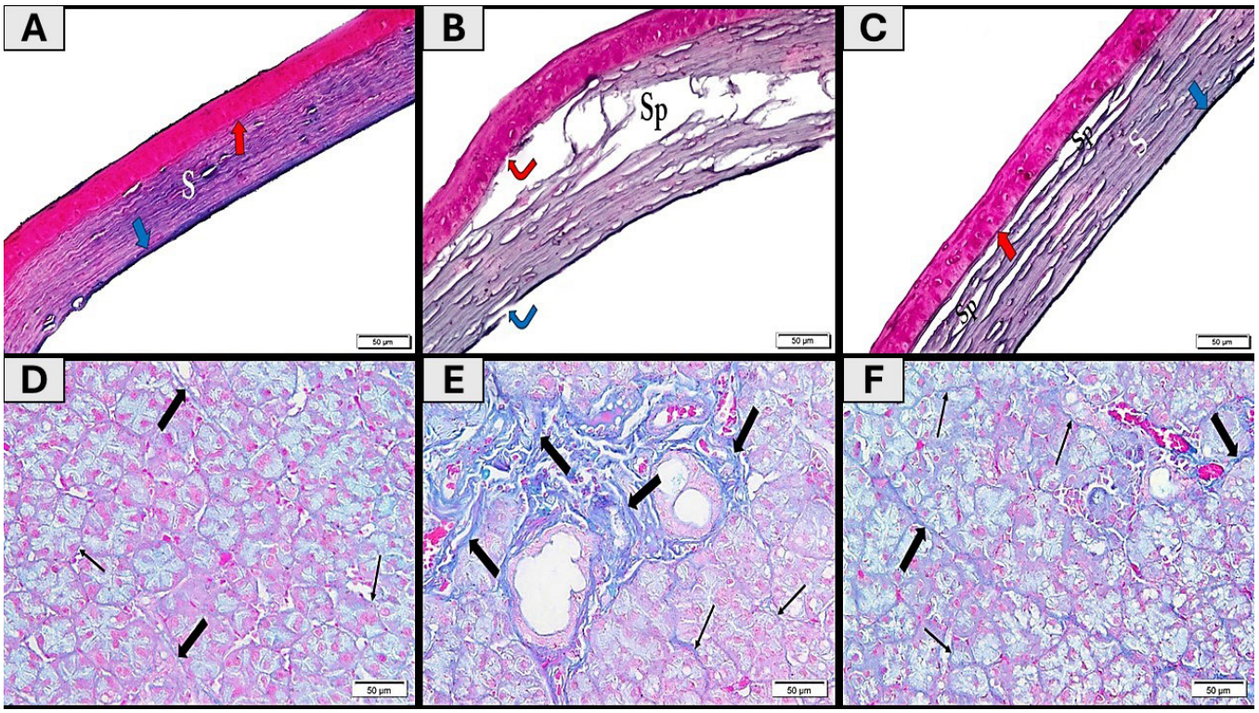

Fig. 4: Photomicrographs of Masson's trichrome stained sections of central cornea and lacrimal glands (x200). (A, D) Group I shows continuous regular basement (red arrow) & Descemet's (blue arrow) membranes. Well-organized collagen bundles within the substantia propria (S) are also observed in cornea. Lacrimal gland shows fine collagen fibers present in the interlobular septa (thick arrows) and between the acini (thin arrows). (B, E) Subgroup II-a exhibits cornea with a discontinuous basement (red right-angled arrow) & Descemet's (blue right-angled arrow) membranes. The substantia propria shows significant disruption and separation of collagen bundles (Sp). The lacrimal gland reveals a marked increase in collagen deposition around the ducts and within the interlobular septa (thick arrows), as well as between the acini (thin arrows). (C, F) Subgroup II-b demonstrates mild separation of collagen bundles (Sp) in substantia propria, in addition to continuous both basement (red arrow) & Descemet's (blue arrow) membranes of the cornea. A mild to moderate deposition of collagen within the septa (thick arrows) and between the acini (thin arrows) is observed in the lacrimal gland.

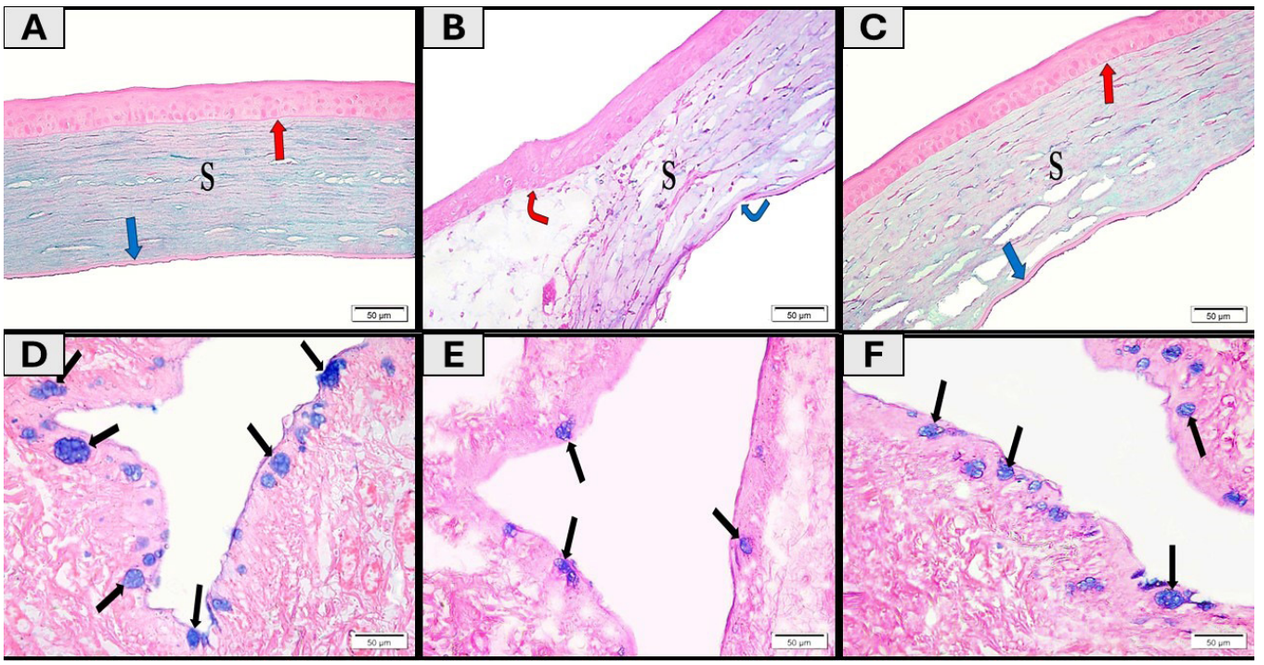

Fig. 5: Photomicrographs of AB-PAS -stained sections of central cornea and conjunctiva (x200). (A, D) Group I shows a strong continuous PAS positive reaction in both basement (red arrow) and Descemet's (blue arrow) membranes with a characteristic magenta red coloration, in addition to a strong AB positive reaction in in the corneal stroma (S) with a bluish-green color. The conjunctiva shows numerous goblet cells (black arrows) within the conjunctival epithelium. (B, E) Subgroup II-a shows an interrupted PAS positive reaction in both basement (red right-angles arrow) and Descemet's (blue right-angled arrow) membranes, accompanied by a weak AB positive reaction in the stroma (S). The conjunctiva shows few goblet cells (black arrows) within the conjunctival epithelium. (C, F) Subgroup II-b shows a strong continuous PAS positive reaction in both basement (red arrow) and Descemet's (blue arrow) membranes with a moderate widespread AB positive reaction in the stroma (S). The conjunctiva shows abundant goblet cells (black arrows) within the conjunctival epithelium.

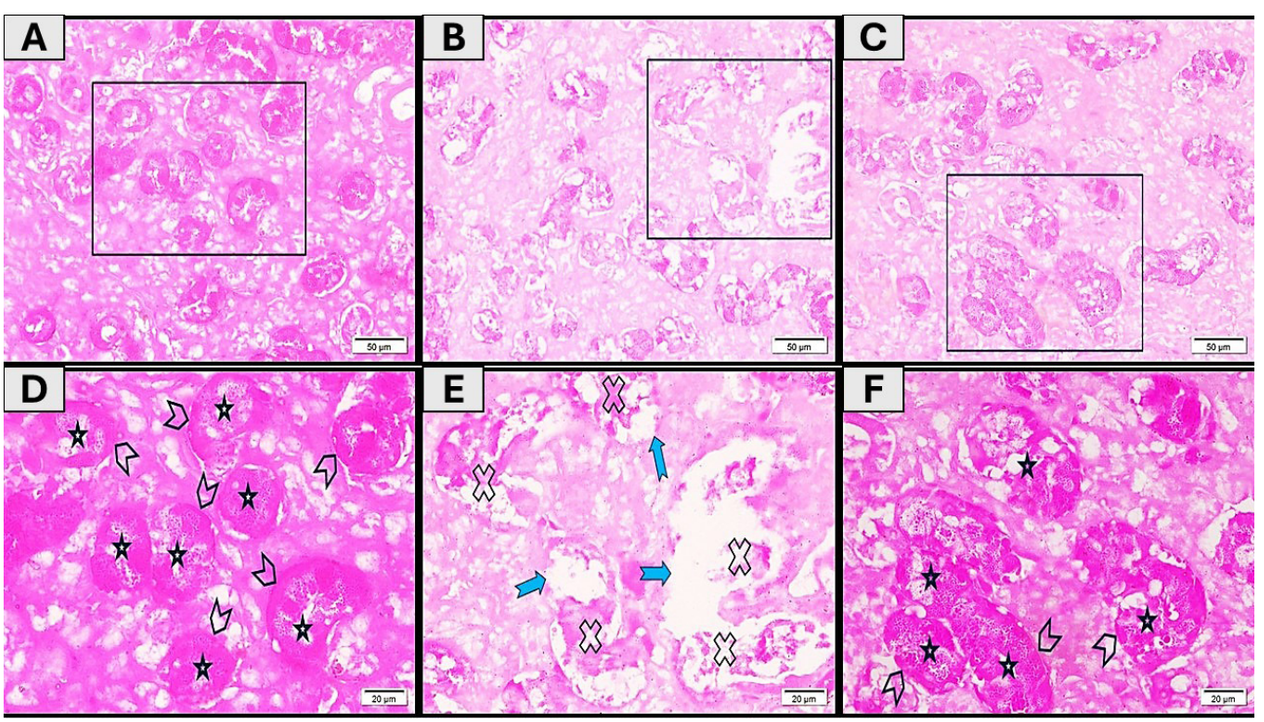

Fig. 6: Photomicrographs of PAS-stained sections of lacrimal gland (A-C x200), (D-F x400). (A, D) Group I shows well-defined acini (square) characterized by strong PAS-positive granules concentrated in the apical cytoplasm (stars) and continuous basement membranes (arrowheads) surrounding these acini. (B, E) Subgroups II-a exhibits numerous distorted acini (square) with sparse PAS-positive granules (X), and discontinuous basement membranes (blue bifid arrows). (C, F) subgroup II-b demonstrates predominantly regenerated acini (square) displaying strong PAS-positive granulation (stars) and intact basement membranes (arrowheads).

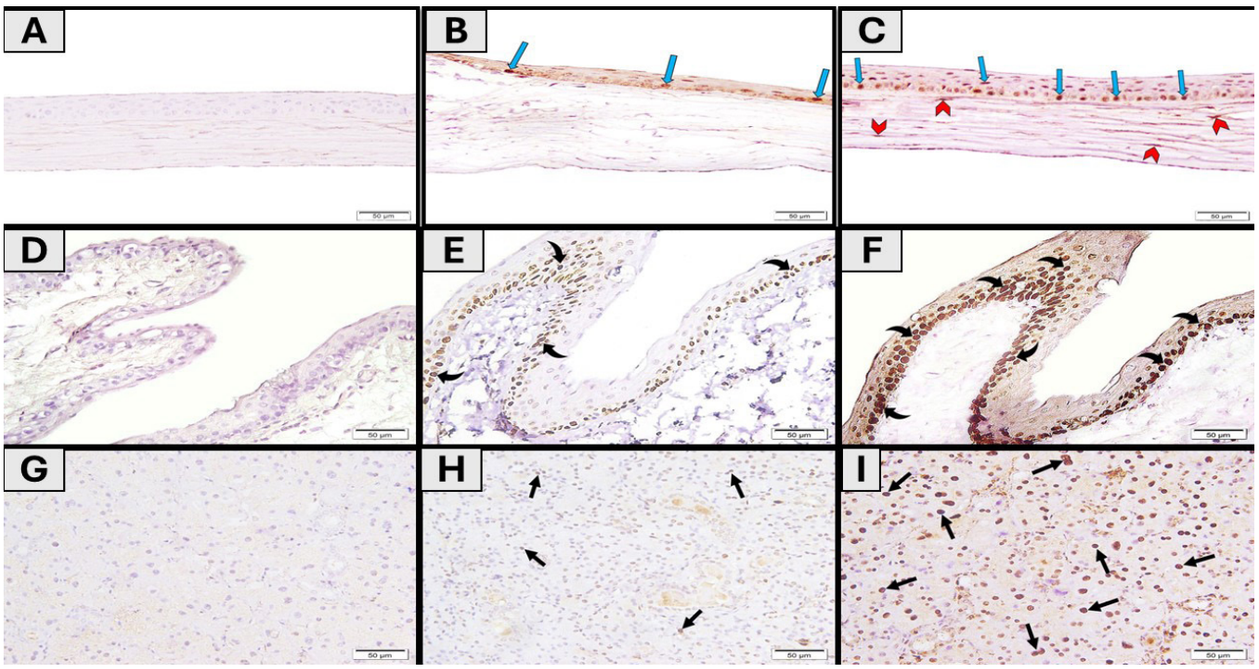

Fig. 7: Photomicrographs of PCNA-stained sections of central cornea, conjunctiva and lacrimal glands respectively (x200). (A, D& G) Group I shows negative immunoreactivity in the cornea, conjunctiva and lacrimal gland. (B, E& H) Subgroup II-a exhibits many PCNA-positive nuclei in basal and supra-basal layers of both corneal (blue arrows) and conjunctival epithelia (curved arrows) and the acinar cells of the lacrimal gland (straight arrows). (C, F& I) subgroup II-b demonstrates numerous positive nuclei in the corneal epithelial layers (blue arrows) and keratocytes (red arrowheads), conjunctival epithelia (curved arrows) and acinar cells of the lacrimal gland (straight arrows).

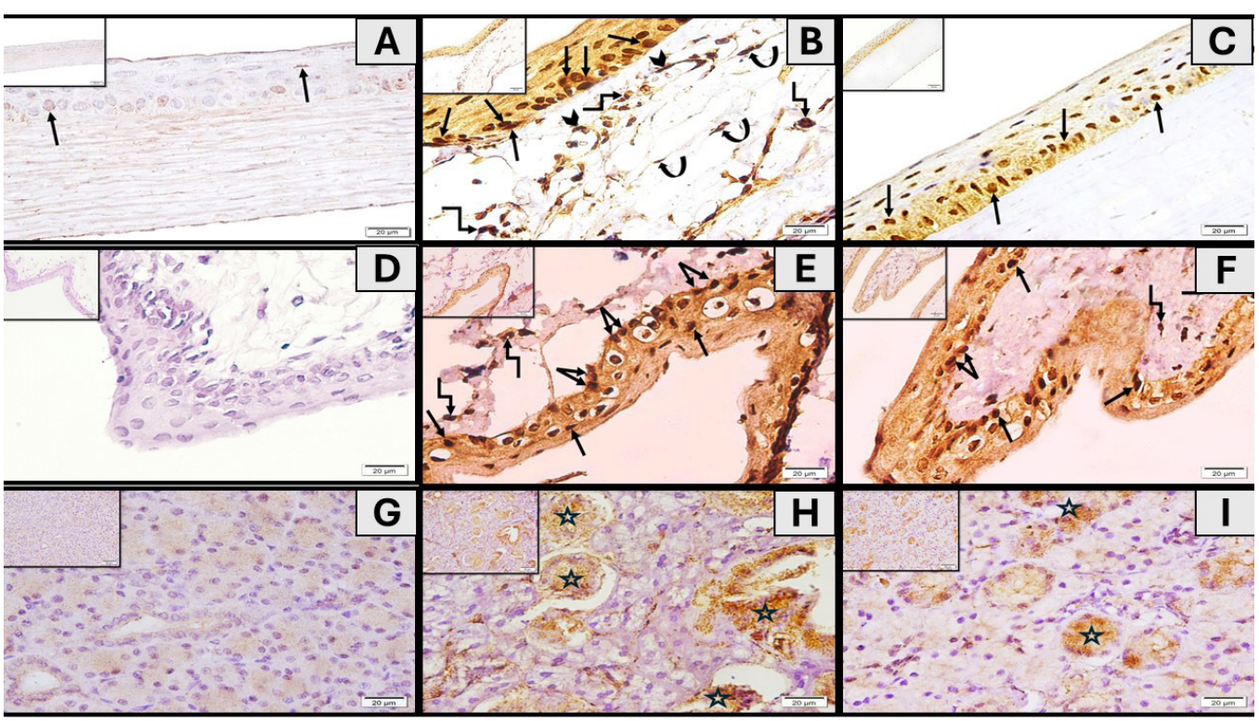

Fig. 8: Photomicrographs of TNF-α stained sections of central cornea, conjunctiva and lacrimal glands respectively (x400), (Inset x200). (A, D& G) Group I shows very faint brown nuclear immunoreactivity in few basal and supra-basal corneal epithelial cells (arrows), while conjunctiva and lacrimal gland shows negative immunoreactivity. (B, E& H) Subgroups II-a exhibits intense brown cytoplasmic and nuclear immunoreactivity within corneal and conjunctival epithelial cells (arrows), stromal keratocytes (curved arrows), vascular endothelial cells (arrowheads), and infiltrating mononuclear cells (right-angled arrows). In addition to strong widespread cytoplasmic immunoreactivity in the acinar cells (stars) of the lacrimal gland. (C, F& I) subgroup II-b demonstrates reduced immunoreactivity in both corneal and conjunctival epithelial cells (arrows) with fewer positive mononuclear cells (right-angled arrows) within the conjunctival stroma, in addition to reduced cytoplasmic immunoreactivity in the lacrimal acinar cells (stars).

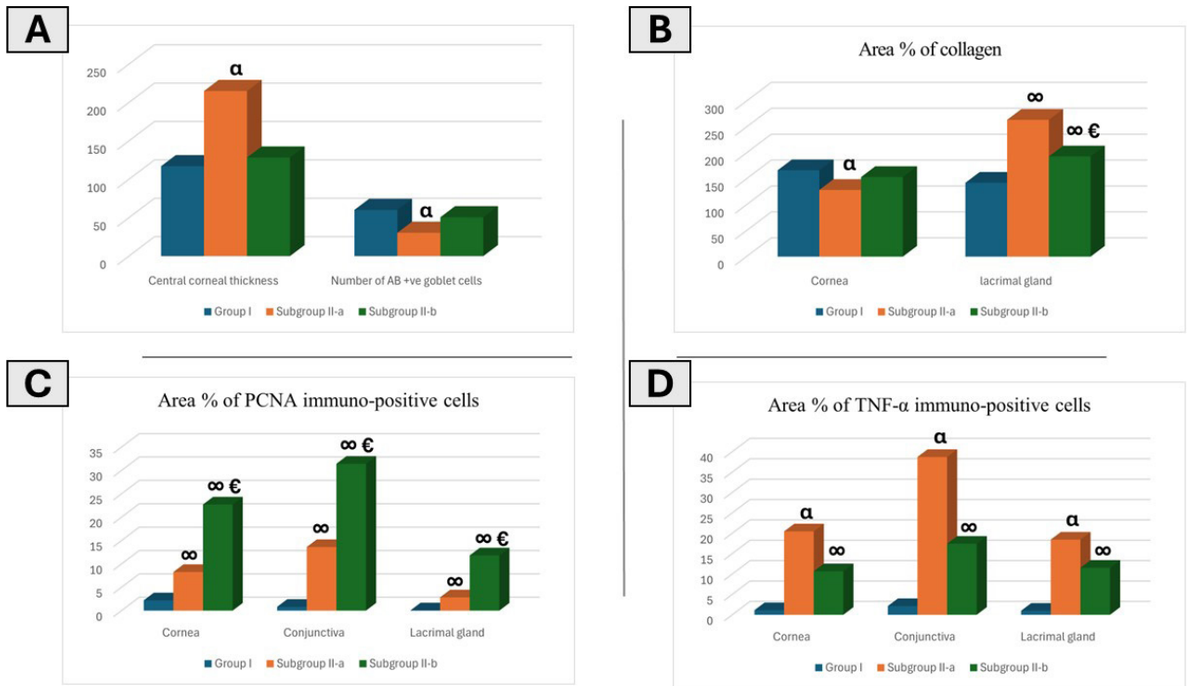

Fig. 9: Histograms of (A) Mean central corneal thickness and mean number AB positive goblet cells. (B) Mean area % of collagen. (C) Mean area % of PCNA immuno-positive cells. (D) Mean area% of TNF-α immuno-positive cells in group I, subgroup II-a and subgroup II-b. (α): significant to group I and subgroup II-b. (∞): significant to group I. (€): significant to subgroup II-a.

DISCUSSION

Dry eye disease (DED) is characterized by tear film instability and ocular surface inflammation[23]. Benzalkonium chloride (BAC) is widely employed to induce DED in animal models for evaluating novel therapeutic approaches[8]. In this study, we investigated the therapeutic efficacy of topical adipose-derived mesenchymal stem cells (ADMSCs) in a BAC-induced dry eye model in male albino rats.

Examination of H&E-stained corneal sections of subgroup II-a (untreated dry eye) revealed significant corneal epithelial damage, characterized by pyknotic nuclei and cytoplasmic vacuolations. Additional findings included epithelial-stromal separation, basement membrane disruption, disorganized stromal collagen with some swollen keratocytes in-between. Focal breaks in Descemet's membrane and endothelial cell loss were also observed, accompanied by a statistically significant increase in corneal thickness compared to control.

These results align with previous studies demonstrating that BAC induced cytotoxicity by disrupting epithelial membranes, compromising basement membranes, and weakening intercellular junctions even at low concentration[8,24]. The resulting oxidative stress and inflammation further exacerbated stromal collagen disarray and keratocyte degenerative changes[25], while endothelial cell damage extended BAC toxicity to the posterior corneal layers[26].

Conversely, subgroup II-b (ADMSCs treated) exhibited partial restoration of corneal architecture. The epithelial layer showed significant repair with minimal residual vacuolated cells and pyknotic nuclei, alongside an intact basement membrane. The substantia propria appeared mostly organized with near-normal keratocytes, and both Descemet's membrane and endothelium were preserved in most regions. Corneal thickness was significantly reduced compared to subgroup II-a.

These reparative effects were consistent with the known mechanisms of ADMSCs, which promoted epithelial and stromal regeneration through differentiation and paracrine secretion of trophic factors. These factors enhanced cell survival, attenuated inflammation, stimulated keratocyte proliferation, and supported extracellular matrix synthesis[6]. Additionally, ADMSC-derived exosomes had been shown to protect and regenerate corneal endothelial cells by reducing senescence and promoting cell cycle progression[27].

In the conjunctiva, subgroup II-a was characterized by disrupted epithelium, significant goblet cell loss, and increased stromal cellular infiltration. These findings were consistent with established BAC-induced conjunctival toxicity, which involved epithelial cytotoxicity, goblet cell depletion, and heightened inflammatory responses mediated by oxidative stress and proinflammatory signaling[28].

ADMSCs treatment (subgroup II-b) ameliorated these changes, restoring epithelial integrity, increasing goblet cell density, and reducing stromal inflammation. This improvement supported the evidence that MSCs could promote epithelial repair, restore goblet cell numbers, and exert anti-inflammatory effects, thereby mitigating BAC-induced conjunctival damage[29].

BAC exposure led to pronounced lacrimal gland damage in subgroup II-a, including acinar distortion, pyknotic nuclei, cytoplasmic vacuolation, ductal epithelial detachment, and vascular congestion. These findings reflected BAC-induced mitochondrial dysfunction, apoptosis, and inflammatory damage, which disrupted glandular architecture and impaired tear secretion[30]. This was consistent with findings from rodent models demonstrating that BAC exposure led to chronic inflammation, acinar cell degeneration, and reduced tear production through oxidative stress and inflammatory cascades[31].

In subgroup II-b, notable restoration of acinar architecture was observed, with most acinar cells regaining normal nuclear morphology. Although some residual damage persisted, including pyknotic nuclei, cytoplasmic vacuolations, and vascular congestion, ductal structures showed partial epithelial reorganization. These findings were supported by recent studies demonstrating that ADMSCs promoted lacrimal gland regeneration and improved glandular architecture after injury or toxic insult[32]. In addition to the immunomodulatory and paracrine actions of ADMSCs, they had been shown to increase vital acinar structures and restore tear secretion in animal models of dry eye disease, confirming their regenerative potential in lacrimal gland dysfunction[33]. The partial persistence of cellular vacuolation and vascular congestion likely reflected ongoing tissue remodeling, consistent with the gradual nature of MSC-based repair[34].

As regards histochemical findings of the corneal sections, Masson's trichrome staining of subgroup II-a revealed marked disruption and separation of collagen bundles and discontinuities in basement and Descemet's membranes supported by a statistically significant decrease in the area % of collagen fibers compared to controls. AB-PAS staining showed interrupted PAS positivity in the membranes and weak AB staining in the stroma, indicated basement membrane disruption and depletion of stromal glycosaminoglycans (GAGs). These changes were consistent with dry eye models, where chronic inflammation-mediated by elevated TNF-α and IL-1β-drived extracellular matrix remodeling and basement membrane breakdown[35]. Additively, upregulation of MMP-9 further contributed to collagen degradation and membrane disruption[36].

Conversely, subgroup II-b displayed mild separation of collagen bundles and restoration of basement and Descemet's membranes, with a significant decrease in collagen area % compared to II-a. AB-PAS staining showed continuous PAS positivity and moderate AB stromal staining, suggesting partial recovery of basement membrane integrity and GAG content, highlighting the ability of stem cell therapy to suppress inflammatory cytokines, inhibit MMPs, and promote extracellular matrix repair[37].

In the conjunctiva, BAC exposure led to a significant reduction in goblet cells and mucin deficiency, as indicated by AB-PAS staining, confirmed by a statistically significant decrease in number of alcian blue positive goblet cells compared to control. This was consistent with dry eye pathology, where inflammation induced goblet cell apoptosis and mucin deficiency[38]. In subgroup II-b, ADMSC treatment restored goblet cell numbers and mucin production, supporting the reparative effect of therapy which can restore epithelial homeostasis and mucin production[6]. This was confirmed by a statistically significant increase in number of alcian blue positive goblet cells compared to II-a. Notably, conjunctival fibrosis was not observed, consistent with previous reports indicating that fibrosis is uncommon in dry eye models without additional injury[39].

In lacrimal glands of subgroup II-a, Masson's trichrome stain showed markedly increased collagen deposition, especially around ducts and within interlobular septa and between acini, confirmed by a statistically significant increase in collagen area %. PAS staining revealed sparse PAS-positive granules and discontinuous basement membranes. Chronic inflammation, driven by cytokines such as TNF-α and IL-1β, led to acinar cell damage, reduced mucin and glycoprotein production (as evidenced by weak PAS staining), and stimulated fibroblasts to produce excess collagen, leading to tissue stiffening and impaired gland function[38,40].

On the other hand, subgroup II-b revealed reduced collagen deposition, with a statistically significant decrease in collagen area % compared to II-a, in addition to strong PAS-positive granules and intact basement membranes. MSCs therapy exerted strong immunomodulatory effects, suppressing these cytokines, thereby attenuating fibroblast activation and collagen deposition[41]. Also, trophic factors and extracellular vesicles secreted by SCs were proved to stimulate proliferation and differentiation of residual epithelial and acinar cells, leading to restoration of normal glandular architecture, enhancing mucin/glycoprotein secretion, and promote basement membrane regeneration[42].

PCNA, a marker of cell proliferation[19], was significantly increased in ADMSC-treated tissues (II-b) compared to untreated DED (II-a) in which PCNA expression was limited to basal epithelial layers and acinar cells, indicating a limited repair response insufficient to restore normal tear secretion[43].

In contrast, subgroup II-b demonstrated widespread PCNA expression throughout the full thickness of the corneal and conjunctival epithelia, signifying robust epithelial proliferation and restoration of barrier function.

This finding was consistent with recent clinical trials of corneal epithelial SC therapy, which reported a 23% improvement in patient symptom scores, attributed to tissue regeneration and inflammation reduction[44]. The marked increase in keratocyte PCNA was likely due to mesenchymal stromal cell (MSC) exosome-mediated delivery of miR-204, which suppressed NLRP3 inflammasome activity and stimulated stromal repair, thereby reducing fibrosis and reactivating dormant keratocytes[45]. Furthermore, the hyperproliferation observed in lacrimal gland acinar cells aligned with recent findings that adipose-derived MSCs enhanced acinar regeneration by upregulating epidermal growth factor (EGF) and fibroblast growth factor 2 (FGF2), effectively reversing glandular atrophy induced by toxic injury[46].

In subgroup II-a, there was intense TNF-α immunoreactivity both in the cytoplasm and nuclei of both corneal and conjunctival epithelial cells, in addition to stromal cells including keratocytes, vascular endothelial cells, and infiltrating mononuclear cells. Similarly, strong widespread cytoplasmic TNF-α was evident in lacrimal gland acinar cells. This marked upregulation reflected the well-documented inflammatory cascade in dry eye disease, where tear hyperosmolarity, microtrauma, and immune activation triggered MAPK and NF-κB pathways, resulting in elevated TNF-α production[47]. TNF-α amplified inflammation by inducing adhesion molecules on endothelial cells, recruiting immune cells, and activating inflammasomes, which exacerbated tissue damage and disrupted the corneal barrier[48].

Conversely, in subgroup II-b, TNF-α expression was moderately decreased and primarily confined to the epithelial layers of both cornea and conjunctiva with reduced stromal involvement, in addition to reduced reactivity in acinar cells of lacrimal glands indicating effective modulation of the inflammatory environment by SC therapy[47]. Localized epithelial TNF-α expression might reflect a controlled response that supported tissue remodeling without promoting chronic inflammation, consistent with evidence that TNF-α inhibition reduceed ocular surface inflammation and improved outcomes in dry eye models[49].

CONCLUSION

In conclusion, the corneal damage detected by fluorescein staining was confirmed thorough histological, immunohistochemical, and statistical analyses. Treatment with topical ADMSCs promoted partial restoration of corneal tissue structure and function, as well as notable improvements in the conjunctiva and lacrimal glands, where inflammation was reduced and tissue regeneration supported. These findings, all confirmed by statistical evidence, highlight the promising potential of ADMSCs as a regenerative therapy for BAC-induced dry eye disease. To further enhance treatment effectiveness, future studies should investigate the benefits of intra-lacrimal stem cell administration to optimize therapeutic outcomes.

CONFLICT OF INTERESTS

There are no conflicts interest.

REFERENCES

1. Huang D and Li Z: Multidimensional immunotherapy for dry eye disease: current status and future directions in Front Ophthalmol (Lausanne). (2024) 4:1449283. doi: 10.3389/fopht.2024.1449283. PMID: 39554604. PMCID: PMC11564177.
2. Goldstein MH, Silva FQ, Blender N, Tran T and Vantipalli S: Ocular benzalkonium chloride exposure: problems and solutions. Eye (Lond). (2022) 36(2):361-368. doi: 10.1038/s41433-021-01668-x. Epub 2021 Jul 14. PMID: 34262161; PMCID: PMC8277985.
3. Kunboon, A, Tananuvat, N, Upaphong, Wongpakaran N and Wongpakaran T: Prevalence of dry eye disease symptoms, associated factors and impact on quality of life among medical students during the pandemic. in Sci Rep. (2024) 14(1):23986. doi: 10.1038/s41598-024-75345-w. PMID: 39402234; PMCID: PMC11473963.
4. Lv Z, Li S, Zeng G, Yao K and Han H: Recent progress of nanomedicine in managing dry eye disease in Adv Ophthalmol Pract Res. (2024) 4(1):23-31. doi: 10.1016/j.aopr.2024.01.008. PMID: 38356795; PMCID: PMC10864857.
5. Surico PL, Barone V, Singh RB, Coassin M, Blanco T, Dohlman TH, Basu S, Chauhan SK, Dana R and Di Zazzo A: Potential applications of mesenchymal stem cells in ocular surface immune-mediated disorders in Surv Ophthalmol. (2024):S0039-6257(24)00083-3. doi: 10.1016/j.survophthal.2024.07.008. PMID: 39097173.
6. Alió Del Barrio JL, De la Mata A, De Miguel MP, Arnalich-Montiel F, Nieto-Miguel T, El Zarif M, Cadenas-Martín M, López-Paniagua M, Galindo S, Calonge M and Alió JL: Corneal Regeneration Using Adipose-Derived Mesenchymal Stem Cells in Cells. (2022) 11(16):2549. doi: 10.3390/cells11162549. PMID: 36010626; PMCID: PMC9406486.
7. Soleimani M, Masoumi A, Momenaei B, Cheraqpour K, Koganti R, Chang AY, Ghassemi M and Djalilian AR: Applications of mesenchymal stem cells in ocular surface diseases: sources and routes of delivery in Expert Opin Biol Ther. (2023) 23(6):509-525. doi: 10.1080/14712598.2023.2175605. PMID: 36719365; PMCID: PMC10313829.
8. Thacker M, Sahoo A, Reddy AA, Bokara KK, Singh S, Basu S and Singh V: Benzalkonium chloride-induced dry eye disease animal models: Current understanding and potential for translational research in Indian J Ophthalmol. (2023) 71(4):1256-1262. doi: 10.4103/IJO.IJO_2791_22. PMID: 37026256; PMCID: PMC10276752.

9. Beyazyıldız E, Pınarlı FA, Beyazyıldız O, Hekimoğlu ER, Acar U, Demir MN, Albayrak A, Kaymaz F, Sobacı G and Delibaşı T: Efficacy of topical mesenchymal stem cell therapy in the treatment of experimental dry eye syndrome model in Stem Cells Int. (2014) 2014: 250230. doi: 10.1155/2014/250230. PMID: 25136370; PMCID: PMC4127226.

10. Linn CL, Webster SE and Webster MK: Eye Drops for Delivery of Bioactive Compounds and BrdU to Stimulate Proliferation and Label Mitotically Active Cells in the Adult Rodent Retina in Bio Protoc. (2018) 8(21):e3076. doi: 10.21769/BioProtoc.3076. PMID: 30687771; PMCID: PMC6347112.

11. Nasser W, Amitai-Lange A, Soteriou D, Hanna R, Tiosano B, Fuchs Y and Shalom-Feuerstein R: Corneal-Committed Cells Restore the Stem Cell Pool and Tissue Boundary following Injury in Cell Rep. (2018) 22(2):323-331. doi: 10.1016/j.celrep.2017.12.040. PMID: 29320729.

12. Srinivas SP and Rao SK: Ocular surface staining: Current concepts and techniques in Indian J Ophthalmol. (2023) 71(4):1080-1089. doi: 10.4103/ijo.IJO_2137_22. PMID: 37026238; PMCID: PMC10276680.

13. Zhang X, M VJ, Qu Y, He X, Ou S, Bu J, Li Y, Wang J, Wu H and Liu Z: Dry eye management: Targeting the ocular surface microenvironment in Int J Mol Sci. (2017) 18(7):1398. doi:10.3390/ijms18071398. PMID: 28661456; PMCID: PMC5535891.

14. Rezapour-Lactoee A, Yeganeh H, Gharibi R and Milan PB: Enhanced healing of a full-thickness wound by a thermoresponsive dressing utilized for simultaneous transfer and protection of adipose-derived mesenchymal stem cells sheet in J Mater Sci Mater Med. (2020) 31(11):101. doi: 10.1007/s10856-020-06433-2. PMID: 33140201.

15. Ma H, Siu WS, Koon CM, Wu XX, Li X, Cheng W, Shum WT, Lau CB, Wong CK and Leung PC: The Application of Adipose Tissue-Derived Mesenchymal Stem Cells (ADMSCs) and a Twin-Herb Formula to the Rodent Wound Healing Model: Use Alone or Together? In Int J Mol Sci. (2023) 24(2):1372. doi: 10.3390/ijms24021372. PMID: 36674885; PMCID: PMC9867064.

16. Francischi JN, Frade TIC, Almeida MPA, Queiroz BFG and Bakhle YS: Ketamine-xylazine anaesthesia and orofacial administration of substance P: A lethal combination in rats in Neuropeptides. (2017) 62:21-26. doi: 10.1016/j.npep.2017.01.003. PMID: 28162846.

17. Kiernan JA: Histological and histochemical methods: Theory and practice. 5th edition. Arnold publisher, London, New York & New Delhi. (2015) pp:132-212.

18. Bancroft, J. D. and Layton, C: "Theory & Practice of histological techniques (7th ed.)", ed. by S. K. Suvarna, C. Layton and J. D. Bancroft, Churchill Livingstone of El Sevier, Philadelphia (2013) pp.173–214.

19. Suvarna SK, Layton C and Bancroft JD: Immunohistochemical and immunofluorescent techniques. In: Bancroft's Theory and practice of histological techniques, chapter 19, 8th edition. Elsevier, China. (2019) pp:337-394.

20. Li DD, Zhang JW, Zhang R, Xie JH, Zhang K, Lin GG, Han YX, Peng RX, Han DS, Wang J, Yang J and Li JM: Proliferating cell nuclear antigen (PCNA) overexpression in hepatocellular carcinoma predicts poor prognosis as determined by bioinformatic analysis in Chin Med J (Engl). (2020) 134(7): 848-850. doi: 10.1097/CM9.0000000000001192. PMID: 33797470; PMCID: PMC8104276.

21. He M, Yang J, Yan S, Shu Q and Liu PC: Conducting a real-world study of Tumor Necrosis factor-alpha inhibitors-induced Systemic Lupus Erythematosus based on the FAERS database in Sci Rep. (2025) 15(1):6838. doi: 10.1038/s41598-025-90566-3. PMID: 40000785; PMCID: PMC11861294.

22. Dalmaijer ES, Nord CL and Astle DE: Statistical power for cluster analysis in BMC Bioinformatics. (2022) 23(1):205. doi: 10.1186/s12859-022-04675-1. PMID: 35641905; PMCID: PMC9158113.

23. Dash N and Choudhury D: Dry Eye Disease: An Update on Changing Perspectives on Causes, Diagnosis, and Management in Cureus. (2024) 16(5):e59985. doi: 10.7759/cureus.59985. PMID: 38854318; PMCID: PMC11162257.

24. Zhang R, Park M, Richardson A, Tedla N, Pandzic E, de Paiva CS, Watson S, Wakefield D and Di Girolamo N: Dose-dependent benzalkonium chloride toxicity imparts ocular surface epithelial changes with features of dry eye disease in Ocul Surf. (2020) 18(1):158-169. doi: 10.1016/j.jtos.2019.11.006. Epub 2019 Nov 15. PMID: 31740391.

25. Pot SA, Lin Z, Shiu J, Benn MC and Vogel V: Growth factors and mechano-regulated reciprocal crosstalk with extracellular matrix tune the keratocyte-fibroblast/myofibroblast transition in Sci Rep. (2023) 13(1):11350. doi: 10.1038/s41598-023-37776-9. PMID: 37443325; PMCID: PMC10345140.

26. Verma L, Malik A, Maharana PK, Dada T and Sharma N: Toxic anterior segment syndrome (TASS): A review and update in Indian J Ophthalmol. (2024) 72(1):11-18. doi: 10.4103/IJO.IJO_1796_23. Epub 2023 Dec 22. PMID: 38131565; PMCID: PMC10841787.

27. Ryu Y, Hwang JS, Bo Noh K, Park SH, Seo JH and Shin YJ: Adipose Mesenchymal Stem Cell-Derived Exosomes Promote the Regeneration of Corneal Endothelium Through Ameliorating Senescence in Invest Ophthalmol Vis Sci. (2023) 64(13):29. doi: 10.1167/iovs.64.13.29. PMID: 37850944; PMCID: PMC10593138.

28. Faria NVL, Sampaio MOB, Viapiana GN, Seabra NM, Russ HH, Montiani-Ferreira F and Mello PAA: Effects of benzalkonium chloride and cyclosporine applied topically to rabbit conjunctiva: a histomorphometric study in Arq Bras Oftalmol. (2019) 82(4):310-316. doi: 10.5935/0004-2749.20190062. Epub 2019 Apr 29. PMID: 31038554.

29. Baudouin C, Denoyer A, Desbenoit N, Hamm G and Grise A: In *vitro* and in *vivo* experimental studies on trabecular meshwork degeneration induced by benzalkonium chloride (an American Ophthalmological Society thesis) in Trans Am Ophthalmol Soc. (2012) 110:40-63. PMID: 23818734; PMCID: PMC3671366.

30. Datta S, Baudouin C, Brignole-Baudouin F, Denoyer A and Cortopassi G: The Eye Drop Preservative Benzalkonium Chloride Potently Induces Mitochondrial Dysfunction and Preferentially Affects LHON Mutant Cells in Invest Ophthalmol Vis Sci. (2017) 58(4):2406-2412. doi: 10.1167/iovs.16-20903. PMID: 28444329; PMCID: PMC5407244.

31. Barros JFF, Sant'Ana AMS, Dias LC, Murashima AAB, Silva LECMD, Fantucci MZ and Rocha EM: Comparison of the effects of corneal and lacrimal gland denervation on the lacrimal functional unit of rats in Arq Bras Oftalmol. (2022) 85(1):59-67. doi: 10.5935/0004-2749.20220008. PMID: 34586229; PMCID: PMC11826637.

32. Surico PL, Scarabosio A, Miotti G, Grando M, Salati C, Parodi PC, Spadea L and Zeppieri M: Unlocking the versatile potential: Adipose-derived mesenchymal stem cells in ocular surface reconstruction and oculoplastics in World J Stem Cells. (2024) 16(2):89-101. doi: 10.4252/wjsc.v16.i2.89. PMID: 38455097; PMCID: PMC10915950.

33. Jaffet J, Mohanty A, Veernala I, Singh S, Ali MJ, Basu S, Vemuganti GK, Singh V: Human Lacrimal Gland Derived Mesenchymal Stem Cells - Isolation, Propagation, and Characterization in Invest Ophthalmol Vis Sci. (2023) 64(10):12. doi: 10.1167/iovs.64.10.12. PMID: 37440263; PMCID: PMC10353750.

34. Dietrich J, Ott L, Roth M, Witt J, Geerling G, Mertsch S and Schrader S: MSC Transplantation Improves Lacrimal Gland Regeneration after Surgically Induced Dry Eye Disease in Mice in Sci Rep. (2019) 9(1):18299. doi: 10.1038/s41598-019-54840-5. PMID: 31797895; PMCID: PMC6892942.

35. Craig JP, Nichols KK, Akpek EK, Caffery B, Dua HS, Joo CK, Liu Z, Nelson JD, Nichols JJ, Tsubota K and Stapleton F: TFOS DEWS II Definition and Classification Report in Ocul Surf. (2017) 15(3):276-283. doi: 10.1016/j.jtos.2017.05.008. Epub 2017 Jul 20. PMID: 28736335.

36. Wang Y, Jiao L, Qiang C, Chen C, Shen Z, Ding F, Lv L, Zhu T, Lu Y and Cui X: The role of matrix metalloproteinase 9 in fibrosis diseases and its molecular mechanisms in Biomed Pharmacother. (2024) 171:116116. doi: 10.1016/j.biopha.2023.116116. Epub 2024 Jan 5. PMID: 38181715.

37. Le Q, Xu J and Deng SX: The diagnosis of limbal stem cell deficiency in Ocul Surf. (2018) 16(1):58-69. doi: 10.1016/j.jtos.2017.11.002. Epub 2017 Nov 4. PMID: 29113917; PMCID: PMC5844504.

38. Bron AJ, de Paiva CS, Chauhan SK, Bonini S, Gabison EE, Jain S, Knop E, Markoulli M, Ogawa Y, Perez V, Uchino Y, Yokoi N, Zoukhri D and Sullivan DA: TFOS DEWS II pathophysiology report in Ocul Surf. (2017) 15(3):438-510. doi: 10.1016/j.jtos.2017.05.011. Epub 2017 Jul 20. Erratum in: Ocul Surf. 2019 Oct;17(4):842. doi: 10.1016/j.jtos.2019.08.007. PMID: 28736340.

39. Barabino S, Chen Y, Chauhan S and Dana R: Ocular surface immunity: homeostatic mechanisms and their disruption in dry eye disease in Prog Retin Eye Res. (2012) 31(3):271-85. doi: 10.1016/j.preteyeres.2012.02.003. Epub 2012 Mar 8. PMID: 22426080; PMCID: PMC3334398.

40. Messmer EM: The pathophysiology, diagnosis, and treatment of dry eye disease in Dtsch Arztebl Int. (2015) 112(5):71-81; quiz 82. doi: 10.3238/arztebl.2015.0071. PMID: 25686388; PMCID: PMC4335585.

41. Kou M, Huang L, Yang J, Chiang Z, Chen S, Liu J, Guo L, Zhang X, Zhou X, Xu X, Yan X, Wang Y, Zhang J, Xu A, Tse HF and Lian Q: Mesenchymal stem cell-derived extracellular vesicles for immunomodulation and regeneration: a next generation therapeutic tool? In Cell Death Dis. (2022) 13(7):580. doi: 10.1038/s41419-022-05034-x. PMID: 35787632; PMCID: PMC9252569.

42. Donthineni PR, Doctor MB, Shanbhag S, Kate A, Galor A, Djalilian AR, Singh S and Basu S: Aqueous-deficient dry eye disease: Preferred practice pattern guidelines on clinical approach, diagnosis, and management in Indian J Ophthalmol. (2023) 71(4):1332-1347. doi: 10.4103/IJO.IJO_2808_22. PMID: 37026265; PMCID: PMC10276701.

43. Zhang Z, Zhang L and Chen B: Characterization of T cells in the progression of dry eye disease using single-cell RNA sequencing in mice in Eur J Med Res. (2025) 30(1):338. doi: 10.1186/s40001-025-02607-2. PMID: 40296131; PMCID: PMC12036131.

44. Rush SW, Chain J and Das H: Corneal Epithelial Stem Cell Supernatant in the Treatment of Severe Dry Eye Disease: A Pilot Study in Clin Ophthalmol. (2021) 15:3097-3107. doi: 10.2147/OPTH.S322079. PMID: 34295148; PMCID: PMC8291803.

45. Jiang Y, Lin S and Gao Y: Mesenchymal Stromal Cell-Based Therapy for Dry Eye: Current Status and Future Perspectives in Cell Transplant. (2022) 31:9636897221133818. doi: 10.1177/09636897221133818. PMID: 36398793; PMCID: PMC9679336.

46. Li C, Li B, Han M, Tian H, Gao J, Han D, Ling Z, Jing Y, Li N and Hua J: SPARC overexpression in allogeneic adipose-derived mesenchymal stem cells in dog dry eye model induced by benzalkonium chloride in Stem Cell Res Ther. (2024) 15(1):195. doi: 10.1186/s13287-024-03815-z. PMID: 38956738; PMCID: PMC11218109.

47. Chu L, Wang C and Zhou H: Inflammation mechanism and anti-inflammatory therapy of dry eye in Front Med (Lausanne). (2024) 11:1307682. doi: 10.3389/fmed.2024.1307682. PMID: 38420354; PMCID: PMC10899709.

48. Wei Y and Asbell PA: The core mechanism of dry eye disease is inflammation in Eye Contact Lens. (2014) 40(4):248-56. doi: 10.1097/ICL.0000000000000042. Erratum in: Eye Contact Lens. 2014 Sep;40(5):311. PMID: 25390549; PMCID: PMC4231828.

49. Ji YW, Byun YJ, Choi W, Jeong E, Kim JS, Noh H, Kim ES, Song YJ, Park SK and Lee HK: Neutralization of ocular surface TNF-α reduces ocular surface and lacrimal gland inflammation induced by in *vivo* dry eye in Invest Ophthalmol Vis Sci. (2013) 54(12):7557-66. doi: 10.1167/iovs.12-11515. PMID: 24052636.

الملخص العربى

دراسة نسيجية حول الفعالية العلاجية المحتملة للخلايا الجذعية الميزنشيمية المشتقة من النسيج الدهني المطبقة موضعيًا في جفاف العين المستحدث تجريبيًا في ذكور الجرذان االبيضاء

أمل احمد فرج[١]، علياء احمد فرج[٢]، أسماء أحمد الشافعي[١]

[١]قسم الهستولوجيا، [٢]قسم طب وجراحة العيون، كلية الطب، جامعة القاهرة، مصر

الخلفية: مرض جفاف العين (DED) هو اضطراب بصري شائع يتميز بعدم استقرار الغشاء الدمعي والالتهاب وتلف سطح العين، مما يؤدي غالبًا إلى عدم الراحة وضعف البصر. تقدم العلاجات الحالية تخفيفًا للأعراض بشكل أساسي، مما يبرز الحاجة إلى حلول علاجية تجديدية.

هدف الدراسة: هدفت هذه الدراسة إلى استكشاف التأثير العلاجي المحتمل للخلايا الجذعية المستخلصة من النسيج الدهني (ADMSCs) عند استخدامها موضعيًا في علاج جفاف العين المستحدث بواسطة كلوريد البنزالكونيوم (BAC) في نموذج الفئران البيضاء الذكور.

المواد والاساليب: تم تقسيم ٣٢ جرذًا ألبينو بالغًا إلى مجموعات تحكم وتجريبية. تم تحفيز جفاف العين باستخدام BAC موضعيًا. تلقت مجموعة العلاج جرعة موضعية من ADMSCs (١ × ١٠^٥ خلية في ٢٥ ميكرولتر) في العين اليمنى مرة يوميًا لمدة أسبوع. تم تقييم تحريض المرض والاستجابة العلاجية عبر تلوين القرنية بفلوريسئين، والفحص النسيجي (تلوين H&E)، وتلوين (AB-PAS) لخلايا الكأس. تم إجراء تحليلات نسيجية مناعية لـ TNF-α وPCNA، إلى جانب تقييمات قياسية وإحصائية

النتائج: أدى تحفيز جفاف العين باستخدام BAC إلى تلف ظهاري قرني كبير، واختلال تنظيم السدى، وتدمير الغشاء القاعدي، وفقدان خلايا الكأس، وتدهور الغدة الدمعية، مصحوبًا بزيادة ترسب الكولاجين وارتفاع تعبير TNF-α. أدى علاج ADMSCs إلى استعادة هيكل القرنية والملتحمة بشكل ملحوظ، وتحسين كثافة خلايا الكأس، وتقليل الالتهاب السدوي، وتعزيز تجديد الأسناخ في الغدة الدمعية. أكد التحليل الكيميائي النسيجي استعادة جزئية لتنظيم الكولاجين ومحتوى الجليكوزامينوجليكان. كشفت النسيجة المناعية عن زيادة تكاثر الخلايا الظهارية والأسناخ (زيادة PCNA) وانخفاض تعبير TNF-α، مما يشير إلى تقليل الالتهاب. أظهر التحليل القياسي تحسنًا كبيرًا في سمك القرنية وعدد خلايا الكأس في مجموعة المعالجة بـADMSCs مقارنة بمجموعة جفاف العين غير المعالجة.

الاستنتاج: العلاج الموضعي بالخلايا الجذعية المستخلصة من النسيج الدهني (ADMSCs) حسّن بشكل فعّال التغيرات النسيجية المرضية الناتجة عن جفاف العين المستحدث بواسطة كلوريد البنزالكونيوم (BAC) لدى الفئران، من خلال تعزيز تجديد الأنسجة وتنظيم الالتهاب. تدعم هذه النتائج إمكانية استخدام ADMSCs كعلاج تجديدي واعد لمرض جفاف العين.